

## Optically detected cyclotron resonance on GaAs/Al<sub>x</sub>Ga<sub>1-x</sub>As quantum wells and quantum wires

D. M. Hofmann, M. Drechsler, C. Wetzel, and B. K. Meyer

*Physikdepartment E 16, Technical University of Munich, James-Franck-Straße, D-85747 Garching, Germany*

F. Hirler, R. Strenz, G. Abstreiter, G. Böhm, and G. Weimann

*Walter-Schottky-Institut, Technical University of Munich, D-85748 Garching, Germany*

(Received 21 December 1994)

GaAs/Ga<sub>x</sub>Al<sub>1-x</sub>As quantum wells and quantum wires were studied by microwave modulation of the photoluminescence (MMPL) and optically detected cyclotron resonance (ODCR). It is shown that the MMPL signal is enhanced under cyclotron resonance conditions of the electrons. The energy transfer to the luminescence is thermal by heating the crystal lattice. The ODCR experiments allowed us to determine selectively the effective masses and mobilities of electrons confined in an 80-Å quantum well, in nominally 80-nm-wide quantum wires prepared by a shallow etching technique structuring the 80-Å quantum well, and an inversion channel formed at a superlattice/buffer layer interface.

### I. INTRODUCTION

Semiconductor samples prepared for the study of low-dimensional phenomena consist in many cases of rather complex layer structures. For example, if quantum wires or quantum dots are the goal, they can be obtained by reducing the dimensionality of a quantum well, but the sample may still contain 2D and of course 3D structures. These structures such as superlattices and buffer layers are necessary due to various reasons, but can complicate the investigations on the object of desire. Investigations on such samples require therefore highly selective characterization methods which have the ability to distinguish between the different structures present in one sample. Cyclotron resonance (CR) can determine carrier properties (effective masses and scattering times) with high precision, but performing conventional CR experiments one may run into problems since the absorption of the microwave (MW) or far-infrared (FIR) power of the whole sample is measured. It can be advantageous to use optically detected cyclotron resonance (ODCR) where the effect of the applied MW- or FIR-power on specific photoluminescence bands is measured.<sup>1,2</sup> Thus it may allow us to separate the carrier properties of different structures present in one sample. Furthermore this method has the potential to obtain enhanced optical resolution compared to photoluminescence (PL) measurements. The MW- or FIR-power absorption of carriers under cyclotron resonance conditions can lead to a selective enhancement or quenching of different recombination channels being unresolved in PL.<sup>3-5</sup> For the energy transfer to the recombining carriers or particles (excitons) two processes are under consideration: (a) impact ionization of bound or localized excitons by free carriers accelerated in the MW field,<sup>4,6-8</sup> and (b) thermal coupling: the accelerated free carriers release energy, i.e. heat, to the lattice

which effects the PL.<sup>9</sup> A way to distinguish between these two processes is to measure the response time of the signals on the applied MW. The optically detected impact ionization (ODII) process is expected to be "fast," i.e., in the order of the lifetime of the recombination (typically 1 nsec in type I quantum wells). The temperature modulation effect was shown to be comparable "slow," in the  $\mu\text{sec}$  range or below.<sup>9</sup> Due to the ODII mechanisms some experiments are quoted in the literature as ODII spectroscopy<sup>4-8</sup> whereas others performing the same experiments call it more generally microwave modulation photoluminescence spectroscopy [MPL or MMPL (Refs. 5 and 9)]. Most of the ODII/MMPL experiments reported so far concentrate on undoped two- or three-dimensional semiconductor structures.<sup>1-14</sup> This is actually another advantage of ODCR spectroscopy compared to standard CR (without illumination of the sample), the photocreation of carriers can substitute the otherwise necessary doping of the material. One task of this paper is to show that the MMPL spectroscopy can also be used for the study of doped semiconductors. In (highly) doped quantum wells the band-band recombination dominates over the excitonic recombination, thus one may expect that the effect of the applied microwaves is dominantly thermal, i.e., heated carriers "modulate" the PL. It may be speculated that this mechanism diminishes the selectivity of the ODCR spectroscopy, because heating of the carriers and the release of the energy to the lattice will heat the complete sample and any of the radiative recombinations is influenced. However, we will show that although the MMPL mechanism is thermal, the ODCR still keeps its selectivity for different carrier gases present in one sample being spatially separated less than 150 nm. The paper is organized as follows: First we describe the MMPL and ODCR features of the quantum well samples prior to the etching process for the quantum wire forma-

tion. These samples have been used to study the MMPL mechanism acting on the quantum well luminescence. Using microwaves (36 GHz) the cyclotron resonance of the GaAs/Al<sub>x</sub>Ga<sub>1-x</sub>As material system occurs naturally at rather low magnetic fields, which allows only a limited resolution, thus we extended the experiments to FIR radiation, which enhances the resolution significantly. The same samples have been used to form quantum wires by lateral modulation of the conduction and valence band caused by holographic lithography and a shallow etching process. The ODCR experiments reveal an increased CR linewidth and increased effective electron mass for the quantum wires compared to the corresponding quantum well, which is an indication for 1D confinement effects.

## II. SAMPLE DESCRIPTION AND EXPERIMENTAL SETUP

The samples used in the experiments were remote doped GaAs/Al<sub>x</sub>Ga<sub>1-x</sub>As single quantum wells grown by molecular beam epitaxy. The layer sequence consists of a 2- $\mu\text{m}$  GaAs buffer layer followed by a 8 times 150- $\text{\AA}$  Al<sub>0.41</sub>Ga<sub>0.59</sub>As/30- $\text{\AA}$  GaAs superlattice. On top of the superlattice, an 80- $\text{\AA}$  GaAs quantum well was grown followed by a 200- $\text{\AA}$  undoped Al<sub>0.41</sub>Ga<sub>0.59</sub>As spacer layer, a 500- $\text{\AA}$   $2 \times 10^{18}\text{-cm}^{-3}$  Si-doped Al<sub>0.41</sub>Ga<sub>0.59</sub>As and a 100  $\text{\AA}$  GaAs cap layer (see Fig. 1). In order to form quantum wires by a lateral modulation of conduction and valence bands, holographic lithography and shallow etching of the doped layer are applied to these quantum well samples. The etching process is stopped inside the Al<sub>x</sub>Ga<sub>1-x</sub>As spacer layer, so that surface defects are separated by more than 100  $\text{\AA}$  from the quantum well. The geometrical width of the wires is approximately 80 nm, the period length 500 nm. For a detailed description of the sample preparation see Ref. 15. For the MMPL and ODCR experiments the sample was placed in a cylindrical open-microwave resonator (TE<sub>011</sub> mode) immersed in liquid helium and working at 36 GHz (8300  $\mu\text{m}$ ) with a maximum power of 500 mW. Usually the power was reduced below 50 mW and amplitude modulated by a *p-i-n* modulator. The resonator is placed in the center of a superconducting split coil magnet generating fields up to 4 T. PL of the sample was excited with the 690-nm line of a

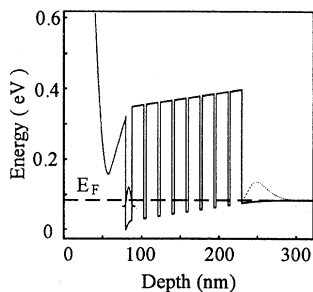


FIG. 1. Schematic conduction band structure of the quantum well samples used in the experiment.

laser diode (5 mW) and spectrally dispersed by a SPEX single monochromator and detected by a photomultiplier. For the ODCR-FIR experiments, the detection system is mainly the same, but the sample is here placed in the center of a solenoid magnet (0–8.0 T) and the exciting and emitted light is guided in an optical fiber. The FIR light (118.8  $\mu\text{m}$ ) with a maximum power of 35 mW (cw) is obtained from a CO<sub>2</sub> pumped Edinburgh Instruments FIR laser; it is amplitude modulated by a mechanical chopper.

## III. RESULTS AND DISCUSSION

### A. Microwave modulated photoluminescence

The PL of the samples was described in detail in Ref. 15, thus we concentrate in this paper on the properties of relevance for the MMPL and ODCR experiments. To illustrate the origin of the two dominant radiative recombinations observable in the quantum well sample (Fig. 2) a self-consistent calculation of the conduction band edge energy for the sample structure described in the previous section is shown in Fig. 1. Electrons are localized in the 80- $\text{\AA}$  quantum well in front of the superlattice and an inversion channel is formed at the interface between the superlattice and the buffer layer. Figure 2(a) shows a PL spectrum. The recombination of the inversion channel is located in the low-energy position and the PL of the 80- $\text{\AA}$  quantum well lies at 1.55 eV. On a logarithmic scale of the PL intensity [inset in Fig. 2(a)] a high-energy tail can be seen with a cutoff at the Fermi energy  $E_F$ . The MMPL spectrum [Fig. 2(b)] reveals additional structure in the inversion channel and the quantum well recombinations. For both PL bands the applied microwaves

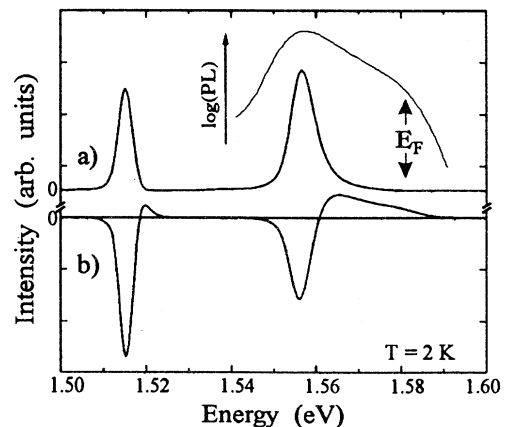


FIG. 2. (a) Photoluminescence spectrum of the remote doped 80- $\text{\AA}$  quantum well sample, showing the recombination due to an inversion channel (low-energy side) and the recombination of the quantum well. The inset shows the quantum well luminescence on a logarithmic scale. (b) Corresponding microwave modulated photoluminescence spectrum (36 GHz, 50 mW,  $T = 2$  K).

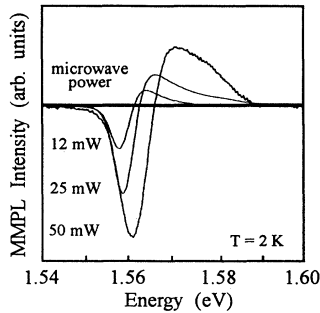


FIG. 3. Microwave modulated photoluminescence spectrum of the recombination of the 80-Å quantum well measured for three different microwave powers.

decrease the PL intensity and weakly increase it on the high-energy side. The MMPL signal intensity of the spectrum in Fig. 2, which is taken at high MW powers, is about 5% of the PL intensity. It should be noted that this is quite low compared to studies on undoped quantum wells, where effects of up to 80% were reported.<sup>6</sup> The energy splitting between the positive and the negative peaks for the quantum well and the inversion channel MMPL strongly depends on the applied MW power. Figure 3 shows the MMPL spectra of the quantum well luminescence measured at various MW powers. Minima and maxima of the signals shift to higher energies with increasing MW powers and also the energy splitting increases with increasing MW power. The MMPL signal intensity increases linearly with increasing MW power. A threshold MW power necessary for the observation of the signal was not observed. The observation of such threshold power would have given evidence that the mechanism causing the MMPL signal is due to impact ionization, as for this mechanism a certain strength of the MW electrical field is required to enable impact ionization of carriers from the valence to the conduction band [1.5 V/cm were measured for the ionization of the excitons in GaAs (Ref. 16)]. Another way to get insight in the mechanism responsible for the MMPL signal is to measure the response on the microwave on/off modulation frequency (Fig. 4). The MMPL signal at 2 K keeps its intensity up to frequencies of about 1 kHz, decreases up to 9 kHz, and is no longer observable at higher frequencies. The decay can be described by an exponential function where the inverse of the frequency response corresponds to a response time of 0.2 msec. DeLong and co-workers<sup>9</sup> have studied various binary and ternary III-V semiconductors and were able to explain the experimentally observed response times down to a few  $\mu\text{sec}$  in a thermal model. Thus also the slow frequency response of the MMPL signal gives evidence that the underlying mechanism for the observation of the MMPL signal is a thermal heating of the lattice. Therefore it is interesting to compare the MMPL spectrum to temperature modulated PL (TMPL) spectra.<sup>5,17</sup> To obtain the TMPL spectrum steady state PL spectra were measured at various temperatures using the same excitation conditions as for the MMPL exper-

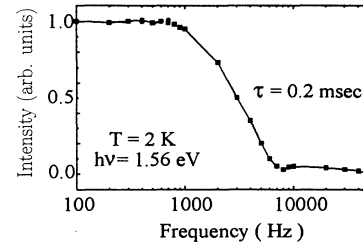


FIG. 4. Frequency response of the microwave modulated photoluminescence signal.

iments. Then, the TMPL spectra were obtained by numerically subtraction of the PL spectra obtained at two different temperatures. The result is shown in Fig. 5, the TMPL spectrum exhibits all features of the MMPL spectra. From a comparison of the intensities of the MMPL and the TMPL signals it is possible to estimate the temperature increase of the sample by the application of the microwaves. It was found that the sample temperature increases about 0.5 K by applying 50 mW MW power.

The frequency response and the power dependence of the MW modulation of the quantum wire luminescence is very similar to that of the quantum well PL. The spectral dependence of the MMPL spectrum in comparison to the PL spectrum of the quantum wire is shown in Fig. 6. Two transitions are observed which have been previously attributed to spatially direct and indirect transitions.<sup>15</sup> The stronger luminescence band on the high energy side of the spectrum is dominantly due to spatially direct  $k$ -conserving transitions of carriers located in the barriers between the quantum wires (see inset in Fig. 6). The linewidth is considerably smaller compared to the quantum well luminescence due to the lower carrier density in the sample caused by the etching for the wire formation which takes partly off the doped layer. The less intense PL band on the low-energy side was attributed to spatially indirect transitions between the conduction band minima and the valence band maxima located in the quantum well region forming the barriers between the wires.<sup>15,18</sup> The indirect luminescence was observed

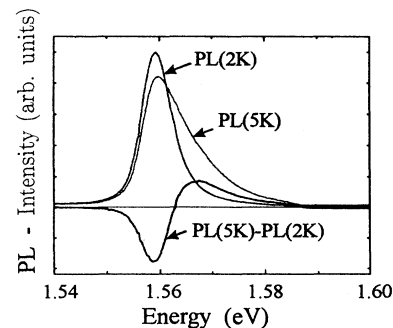


FIG. 5. Photoluminescence spectra of the 80-Å quantum well taken at two temperatures (2 and 5 K) and spectra obtained by numerical subtraction.

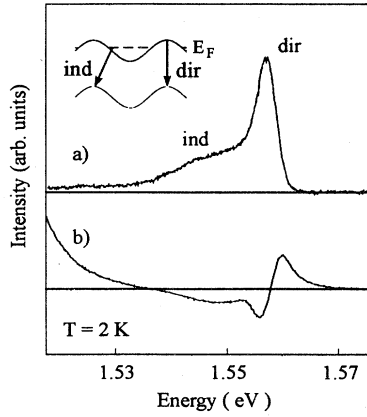


FIG. 6. (a) Photoluminescence spectrum of the quantum well sample after the etching process for the wire formation. The inset shows schematically the potential modulation of the valence and conduction bands in the quantum well and related direct and indirect photoluminescence transitions. (b) Corresponding microwave modulated photoluminescence spectrum.

to shift with decreasing excitation density towards lower energies. This was explained by the separation of photoexcited carriers which modifies the built-in lateral potential. An increasing illumination density generates a higher density of electrons and holes. The separation of these carriers leads to a flattening of the modulation due to electrostatic screening. The effective band gap for the indirect transition increases and as a consequence the indirect transition shifts, while the direct transition is almost unaffected. The direct luminescence of the quantum wire exhibits a derivative line shape in the MMPL spectrum. The indirect transition shows only a decreasing PL intensity upon the application of microwaves. The increase of the MMPL spectrum at the low-energy side is caused by the intense MMPL signal of the inversion channel recombination.

As in the case of the quantum well luminescence, the line shape of the MMPL spectrum of the quantum wire can be well described by the temperature derivative of the PL spectrum.

### B. Optically detected cyclotron resonance

The dependence of the MMPL signal intensity on an external magnetic field is shown in Fig. 7(a). For the inversion channel PL as well as for the quantum well luminescence the line shape of the MMPL signal as a function of the magnetic field is that of a partly resolved cyclotron resonance. The MMPL signal is not observable at magnetic fields above 0.3 T. To confirm this observation we performed similar experiments using the FIR-laser instead of the microwaves [Figs. 7(b) and 7(c)]. For the inversion channel PL an extremely narrow cyclotron resonance is observed [Fig. 7(b)]; For the quantum well PL the resonance is broader [Fig. 7(c)]. Under resonance

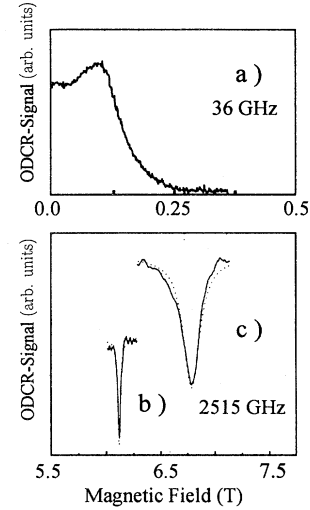


FIG. 7. Optically detected cyclotron resonance spectra observed: (a) on the quantum well luminescence using microwaves; (b) observed on the inversion channel recombination using far infrared (FIR) radiation; and (c) on the quantum well using FIR radiation.

condition the FIR frequency  $\omega_0$  equals the cyclotron angular frequency  $\omega_c = eB/m^*$ , where  $e$  is the elementary charge,  $B$  the magnetic field, and  $m^*$  the effective mass. Fits to the resonance lines [dashed lines in Figs. 7(b) and 7(c)] using the following equation:<sup>19</sup>

$$P \propto \frac{1 + (\omega_0^2 + \omega_c^2)\tau^2}{[1 + (\omega_c^2 - \omega_0^2)\tau^2]^2 + 4\omega_0^2\tau^2} \frac{Ne^2\tau}{m^*}, \quad (1)$$

where  $\tau$  is the carrier momentum relaxation time,  $P$  the power absorbed and  $N$  the number of carriers, give for the resonance of the inversion channel an effective mass

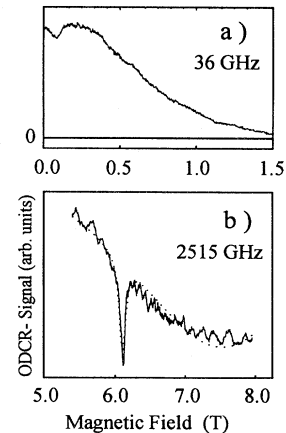


FIG. 8. Optically detected cyclotron resonance spectra observed on the quantum wire luminescence: (a) using microwaves; (b) far-infrared radiation.

of  $m^* = 0.068 \pm 0.001 m_0$ . A mobility can be deduced from the resonance halfwidth at half maximum. For the inversion channel it is  $\mu_{CR} = e\tau/m^* = 380\,000 \pm 3000 \text{ cm}^2/\text{Vs}$ . On the quantum well PL  $m^* = 0.075 \pm 0.002 m_0$  and  $\mu_{CR} = 60\,000 \pm 3000 \text{ cm}^2/\text{Vs}$  are observed. The  $m^*$  value observed on the inversion channel PL is close to the value of electrons in bulk GaAs, the difference to the effective mass of the electrons in the quantum well can be explained by quantization and non-parabolicity effects which increase  $m^*$ .<sup>20</sup> The 2D nature of both resonances is proven by their variation with the magnetic field orientation, which shows the typical cosine behavior.<sup>20,21</sup> The effective mass values determined by ODCR are in good agreement to data obtained by magnetotransport and Shubnikov-de Haas measurements, however, the mobilities are about a factor of 2 lower compared to those investigations.<sup>22</sup> The reason is not completely understood but it may be due to the higher optical and MW excitation densities used for the ODCR experiment which may cause additional scattering. Using the data obtained by the FIR-ODCR experiments and calculating the expected resonance position and linewidth for the microwave experiment the observed field position and line shape is reproduced. The difference in  $m^*$  for the inversion channel compared to the quantum well is not resolvable in the microwave experiment. It should be noted that by fixing the magnetic field at resonance position in the FIR-ODCR experiment and scanning the optical detection wavelength similar spectra are obtained as in the MMPL experiment using microwaves.

In contrast to the quantum well the microwave ODCR signal measured on the quantum wire PL is extremely broad and is detectable for fields up to 1.3 T [see Fig. 8(a)]. At low fields the inversion channel resonance is weakly superimposed. Assuming that the broad structure is due to a cyclotron resonance, a best fit gives  $m^* = 0.080 \pm 0.004 m_0$  and  $\mu_{CR} = 8000 \pm 3000 \text{ cm}^2/\text{Vs}$ . Again the FIR-ODCR experiment was helpful to convince us that such a broad structure indeed originates from a cyclotron resonance [Fig. 8(b)]. A signal is found in the field range from 5.0 to 8.0 T, superimposed is the narrow inversion layer resonance at 6.2 T. The dashed line in Fig. 8(b) shows a calculation of the resonance position and half width expected for the FIR-ODCR signal using the data obtained from the microwave experiments. The resonance is expected to have its maximum at 7.5 T with a half width of about 2 T. Thus in the FIR-ODCR experiment only the low-field side could be detected due to the limited strength of the magnetic field available for the experiments.

Upon variation of the angle between the sample normal and the magnetic field direction the cyclotron resonance measured on the quantum wire PL shows a similar 2D behavior as the resonances of the inversion channel

and the quantum well. The resonance position shifts to higher field values and the linewidth broadens due to increasing interface scattering. For angles between the magnetic field and the normal perpendicular to the sample surface larger than  $30^\circ$ , the resonance structure vanishes completely and only a field independent signal is detected. Different ODCR features dependent on whether the wires are oriented parallel or perpendicular to the magnetic field, as observed recently in serpentine superlattice quantum wire arrays,<sup>23</sup> could not be observed. However, the geometrical width of the wires studied in that work was considerably smaller than the width of the wires studied here. The cyclotron orbit parameter in our MW experiments is about 150 nm, which is significantly larger than the width of the quantum wires. Thus we did not expect to observe 1D quantization effects in these experiments. The potential modulation may only introduce additional scattering, explaining the decrease in mobility.

The FIR-ODCR experiments are more suitable to reveal such effects as the cyclotron orbit shrinks to 20 nm. It was shown that the modulation of a quantum well potential by a one-dimensional, harmonic potential  $V(x) = V_0 \cos(kx)$ ,  $k = p/a$  ( $a$  is the period length) leads to a broadening of the Landau levels into Landau bands.<sup>24,25</sup> The broadening depends on the Landau level number and causes an increasing CR linewidth and, depending on the Fermi level position, an increased resonance position. Both effects are observed in our ODCR experiments which can be taken as evidence that 1D confinement effects are indeed observed. However, to date more quantitative statements are not possible; experiments using higher magnetic fields are necessary.

#### IV. CONCLUSIONS

It has been shown that cyclotron resonance of electrons enhances the microwave modulated photoluminescence signal in doped GaAs/Al<sub>x</sub>Ga<sub>1-x</sub>As quantum well and quantum wire samples. The energy transfer to the luminescence is a slow process via heating of the lattice. However, this optical detection of cyclotron resonance enables the selective determination of the effective masses and carrier mobilities on the radiative recombinations of the quantum well, the quantum wire and an emission of an inversion channel induced at the Al<sub>x</sub>Ga<sub>1-x</sub>As/GaAs superlattice.

#### ACKNOWLEDGMENT

The authors would like to thank the Deutsche Forschungsgemeinschaft for financial support.

<sup>1</sup> P.G. Baranov, Yu.P. Veshchunov, R.A. Zhitnikov, N.G. Romanov, and Yu.G. Shreter, Pis'ma Zh. Eksp. Teor. Fiz. **26**, 3699 (1977) [JETP Lett. **26**, 249 (1977)].

<sup>2</sup> R. Romestain and C. Weisbuch, Phys. Rev. Lett. **5**, 2067

(1980).

<sup>3</sup> B.M. Ashkinadze, V.V. Belkov, and A.G. Krasinskaya, Fiz. Tekh. Poluprovodn. **24**, 883 (1990) [Sov. Phys. Semicond. **24**, 555 (1990)].

- <sup>4</sup> M. Godlewski, K. Frone, M. Gajewska, W.M. Chen, and B. Monemar, *Phys. Rev. B* **44**, 8357 (1991).
- <sup>5</sup> B.M. Ashkinadze, E. Cohen, A. Ron, and L. Pfeiffer, *Phys. Rev. B* **47**, 10 613 (1993).
- <sup>6</sup> F.P. Wang, B. Monemar, and M. Ahlström, *Phys. Rev. B* **39**, 11 195 (1989).
- <sup>7</sup> H. Weman, M. Godelewski, and B. Monemar, *Phys. Rev. B* **38**, 12 525 (1988).
- <sup>8</sup> D. Dedulewicz and M. Godlewski, *Acta Phys. Pol. A* **84**, 535 (1993).
- <sup>9</sup> M.C. Delong, I. Viohl, W.D. Ohlsen, P.C. Taylor, and J.M. Olson, *Phys. Rev. B* **43**, 1510 (1991).
- <sup>10</sup> A. Moll, C. Wetzel, B.K. Meyer, P. Omling, and F. Scholz, *Phys. Rev. B* **45**, 1504 (1992).
- <sup>11</sup> P. Emanuelsson, M. Drechsler, D.M. Hofmann, A.L. Efros, B.K. Meyer, and B. Clerjaud, *Solid State Commun.* **90**, 635 (1994).
- <sup>12</sup> P. Emanuelson, M. Drechsler, D.M. Hofmann, B.K. Meyer, M. Moser, and F. Scholz, *Appl. Phys. Lett.* **64**, 2849 (1994).
- <sup>13</sup> B.C. Cavenett and E.J. Pakulis, *Phys. Rev. B* **32**, 8449 (1985).
- <sup>14</sup> E.J. Pakulis and G.A. Northrop, *Appl. Phys. Lett.* **50** 1672 (1987).
- <sup>15</sup> F. Hirler, R. Strenz, R. Kuchler, G. Abstreiter, G. Böhm, J. Smoliner, G. Tränkle, and G. Weimann, *Semicond. Sci. Technol.* **8**, 617 (1993).
- <sup>16</sup> W. Bludau and E. Wagner, *Phys. Rev. B* **13**, 5410 (1976).
- <sup>17</sup> M. Gal, Z.Y. Xu, F. Green, and B.F. Usher, *Phys. Rev. B* **43**, 1546 (1991).
- <sup>18</sup> F. Hirler, Dissertation, Technische Universität München, Germany, 1994.
- <sup>19</sup> L.D. Lassnig, *Phys. Rev. B* **31**, 8076 (1985).
- <sup>20</sup> G. Bastard, *Wavemechanics Applied to Semiconductor Heterostructures* (Les Edition Physique, Paris, 1988).
- <sup>21</sup> B. Lax and J.G. Mavroides, *Solid State Phys.* **11**, 261 (1960).
- <sup>22</sup> C.M. Engelhardt (private communication).
- <sup>23</sup> K. Swiatek, H. Weman, M.S. Miller, P.M. Petroff, and J.L. Merz, *Acta Phys. Pol. A* **83**, 583 (1993).
- <sup>24</sup> R.W. Winkler, J.P. Kotthaus, and K. Ploog, *Phys. Rev. Lett.* **62**, 1177 (1989).
- <sup>25</sup> A.V. Chaplik, *Solid State Commun.* **53**, 539 (1985).